Preprints (www.preprints.org) | NOT PEER-REVIEWED | Posted: 4 December 2018 doi:10.20944/preprints201812.0038.v1

Article

Speleothem stable isotope records from Eastern Europe & Turkey

Zoltán Kern[1*], Attila Demény[1], István Gábor Hatvani[1]

[1] Institute for Geological and Geochemical Research, Research Centre for Astronomy and Earth Sciences, Hungarian Academy of Sciences, H-1112 Budapest, Hungary; kern.zoltan @mta.csfk.hu, hatvaniig@gmail.com

* Correspondence: kern.zoltan@mta.csfk.hu; Tel.: +36-70-253-8188

Academic Editor: name

Received: date; Accepted: date; Published: date

Abstract: The region of Eastern Europe & Turkey contributed to the SISAL (Speleothem Isotopes Synthesis and AnaLysis) global database with stable carbon- and oxygen isotope time-series from 18 entities from 14 cave systems. The currently available oldest record from this region is the ABA-2 flowstone record (Abaliget Cave; Hungary) reaching back to MIS 6. The temporal distribution of the compiled 18 entities points out a ~20-kyr-long period, centering around 100 ka, lacking speleothem stable isotope record in the region. The regional subset of SISAL_v1 records displays a continuous coverage for the past ~90 kyr for both $\delta^{18}O$ and $\delta^{13}C$, with a mean temporal resolution of ~12 yr for the Holocene, and >50 yr for the pre-Holocene period. The highest temporal resolution both for the Holocene and the pre-Holocene was achieved in the So-1 record (Sofular Cave; Turkey). Assessing the data, an important split was found regarding the climatic interpretation of speleothem $\delta^{18}O$. While the oxygen isotope composition of more continental formations is thought to reflect mainly temperature variations and changes in moisture transport trajectories, it may strongly reflect fluctuations of precipitation amount in the southern part of the region. Variations of $\delta^{13}C$ primarily interpreted as humidity changes reflecting dry/wet periods across the region. Elevation gradients from three non-overlapping time periods from the region - for the last 5kyr - indicated systematically prevailing elevational gradients around -0.26‰ 100m^{-1} in $\delta^{18}O$. The regional comparison of SISAL_v1 speleothem $\delta^{18}O$ and the temporal distribution of coarsely crystalline cryogenic cave carbonate occurrences back to 45ka does not appear to confirm the finding that occurrence of the latter coincides with the warming from stadial to interstadial conditions.

Keywords: Carpathians, Balkan Peninsula, Holocene, hydroclimate, cryogenic cave carbonate, carbon, oxygen

1. Introduction

South-eastern Europe is the cradle of karst research [1-3]. The Kras Mountains in Slovenia gave their name to the entire discipline, and the very first karst research [4] and speleological [5] institutes were established in this region. Eastern Europe and Turkey has a very diverse karst landscape, and wide range of geochronological and geochemical investigations targeted the cave deposits in this region, aiming to infer information about past environments.

Radiometric dating of submerged speleothems from the Dalmatian Coast helped to constrain periods of sea-level low- [6-8] and high-stands [9] during the Quaternary.

Trace element variability in speleothems from the region provided basis for paleohydroclimate implications [10-12], supported the identification of historical flood events [13]. Siklósy et al. [14] associated a sudden rise in rare earth elements with the Middle Bronze Age eruption of Santorini. In

Preprints (www.preprints.org) | NOT PEER-REVIEWED | Posted: 4 December 2018 doi:10.20944/preprints201812.0038.v1

the meanwhile, changes in U concentration and $\delta^{234}U$ changes associated with an increase in detrital material (e.g. Al, Si, Th) in the younger part of the same flowstone were used to detect pollution from historical mining activity [15]. Geochemical imprint (e.g. peaks in Br, Mo, S) was found to be indicative for the Minoan eruption studying the trace element profile in the So-1 record from Sofular Cave [16].

Although it has been long recognized that stable isotope analysis of inclusion-hosted water has a great potential in speleothem-based paleoclimate reconstructions [17], the relatively large sample amount required for classical dual inlet mass spectrometry and the sophisticated technique for O isotope analysis (using fluorine compounds as reagents) precluded wide application. With the advent of continuous flow mass spectrometry and laser spectroscopy, the required sample volume has decreased significantly and coupled analysis of H and O isotope compositions of inclusion-hosted water became easily available, for details see [18]. Despite the potential of inclusion fluid research, stable isotope compositions of fluid inclusions have only been gathered from Turkish and Hungarian speleothems from the Eastern Europe & Turkey region. Hydrogen isotope compositions of inclusion-hosted water, analyzed by the continuous flow technique [19] for a stalagmite from SE Hungary was interpreted as a sign of drip water composition variation in the Bronze Age [14]. Although the analytical precision and post-deposition exchange processes precluded precise paleotemperature calculations, the co-variation of $\delta^{18}O$ for speleothem calcite and inclusion-hosted water analyzed in a stalagmite from Eastern Turkey were used to infer past variations in seasonal precipitation distribution [20]. Mid-Holocene changes in moisture transport trajectories were inferred from the H isotope compositions of inclusion-hosted water analyzed by conventional dual inlet mass spectrometry [21]. An important methodological recognition is that hydrogen isotope compositions provide reliable paleoclimate records, while $\delta^{18}O$ data are compromised due to post-deposition recrystallization and calcite-water isotope exchange [22]. As a result, δ^2H values were used for paleotemperature calculations either applying local δ^2H-temperature relationships, or combining the δ^2H data with calcite $\delta^{18}O$ values [11,18]. These procedures yielded paleotemperature estimates in agreement with independent methods both for the last interglacial [18] and the Middle Bronze Age [11].

Although the longest history of karst research leads back to this region [1], stable isotope investigations of calcareous speleothems began relatively late, at the very end of the 20th century [23,24]. Stable isotope ratios of certain non-calcareous cave deposits, such as cave ice [25,26] and guano deposits [27-29], have a pronounced paleoclimatological potential in the region, however stable carbon and oxygen isotope ratios of carbonate deposits became the most frequently investigated and most abundant geochemical parameter in speleothems studies in Eastern Europe and Turkey.

The first studies aimed to infer paleoenvironmental reconstructions based on stable isotope composition of Late Pleistocene speleothems were carried out in Wierna Cave, Southern Poland [23] and Ceremosnja Cave (Serbia) [30]. Nevertheless, this aim was first achieved in Bear's Cave (Pestera Urşilor), Romania [31]. Several other records followed these within a short time from the same area (e.g. [14,32,33]); including the iconic So-1 record from Sofular Cave, Northern Turkey [34] which provided the first speleothem-based climate record covering the Holocene and the Last Glacial in SE Europe.

The Eastern Europe & Turkey SISAL region is an important hydroclimatological transition zone. The study area lies in the temperate climate zone [35], but is characterized by a highly diverse precipitation regime. The extreme humid conditions along the coastal areas of the Dinaric Karst (annual precipitation >4000 mm) to the arid conditions in central Anatolia (annual precipitation <300 mm) both hosting extended karstic terrains. Accurately dated and robust terrestrial hydroclimate records, such as those provided by speleothems offer an excellent way to reconstruct the changes in hydroclimate on decadal to orbital time scales. Moreover, a long-term perspective of (hydro)climate variability for the Eastern Europe & Turkey SISAL region provides an important context for evaluating potential shifts in large-scale atmospheric moisture-flux conditions, since this

 doi:10.20944/preprints201812.0038.v1

is the only region of the continent where the contribution of Mediterranean sourced moisture year-round exceeds ~20% [36].

The present paper describes and evaluates the spatiotemporal coverage of the speleothem derived stable isotope records for the last 160,000 yrs as available in the SISAL_v1 database [37]. The paper highlights the areas and periods lacking data and how these might be mitigated taking additional identified records into consideration for the Eastern Europe and Turkey region. The number of overlapping records is low in general, except for 1-6 ka (5<n<8), when the spatial distribution and the temporal coverage provided the opportunity to explore the spatial pattern of stable oxygen isotope composition of speleothem calcite ($\delta^{18}O_{spel}$). In addition, the negative extremes of $\delta^{18}O_{spel}$ are compared to the cumulated probability of the ages of coarsely crystalline cryogenic cave carbonates (approx. 10-45 ka) to gain excess knowledge about the paleoenvironment, because the two types of secondary cave carbonates have totally different origins.

2. Study Region and Climate

Karst areas occupy ~50% of the Eastern Europe & Turkey SISAL region (3.03×10^6 km^2). These karst areas can be categorized into three types based on relief and climate characteristics [38]:

- High range mountains, including the Dinarides and Hellenides, the high elevation areas of the Carpathians ,and the northern and southern mountains of Anatolia (Taurides, Pontides),
- Mediterranean medium range mountains, in some parts of southern Dalmatia and surrounding the Aegean Sea and extending to central Anatolia,
- Humid hills and plains. This is the dominant karstic landscape of the Carpathians, NW part of the Dinarides, N and W part of Black Sea coast areas and all the karst NW from the Carpathians up to the Baltic Coast.

The southern regions, from the Dalmatian Coast through the Peloponnesus and large part of Anatolia are dominated by Mediterranean climate characterized by dry, hot summers (minimum precipitation < 40mm, mean temperature of the warmest month (Tmax) ≥ 22°C) and warm (Tmax<22°C and at least 4 monthly avg. temperature (T) ≥ +10°C) summers ([35]). Most of the region is characterized by wet continental or boreal climate (Figure S1). Continentality increases eastwards. Warm temperate/continental climate (monthly mean temperature of the coldest month (Tmin) is between -3 and 18°C) with warm summers and no dry season prevails over the elevated terrains of the Balkan Peninsula stretching northward to the Baltic Coast. In the meanwhile, areas with warm temperate hot summers occur in the Central Balkan region and the south-eastern part of the Eastern European Plains.

Boreal climate with warm summers without a dry season prevails over large part of the mountainous area (Carpathians, Dinarides, and Trachian Massive) and the northeastern parts of the Eastern European Plains up to the Gulf of Finland. The appearance of its counterpart with cool summers and cold winters (Tmax< +22°C, the 4 monthly avg. T < +10°C and Tmin > -38°C) is restricted to the highest regions of the Carpathian Range (Figure S1).

From a seasonal perspective, warm season cyclones reach the Baltic countries originating from the Mediterranean- and Black seas, as well as from the North Atlantic. Cold season cyclones, however, originate almost exclusively from the North Atlantic [39]. Mediterranean moisture is the dominant source for precipitation in the Balkan Peninsula [40,41]. The Black Sea acts as an important moisture source for the surrounding coastal region and for Northern Turkey [34,42].

The highly elevated mountainous areas show the largest recharge volumes (700-800 mm a-1), however in percentage recharge rate is higher in the Mediterranean regions (from ~20% to ~65%) than in the high range mountains (from ~5% to ~65%). The recharge rate of the humid hills and plains varies between ~5% and ~60% with a mean of ~30%, being lower than in the Mediterranean medium range mountains and high range mountains [38]. Overall, it can be said that in the Eastern Europe & Turkey SISAL region, the maximum recharge rates can be observed in the Dinaric karst and Western Anatolia, while the Eastern Balkan and central-east Anatolia has the driest karstic areas [38].

 doi:10.20944/preprints201812.0038.v1

3. "Eastern Europe & Turkey" Records in SISAL_v1

3.1 Distribution of speleothem isotopic records in space and time

The Dinaric Karst is underrepresented in the SISALv1 database (Figure 1; Table 1), despite its richness in caves and cave sediments. There is a 54-yr-long modern speleothem from Postojna Cave [24] and a ca. 1700-yr long stalagmite from the Modrič Cave [43] from the Dinaric region. There are three records in the SISALv1 from two caves located in the Peloponnesus (Mavry Trypa Cave [44]; Kapsia Cave [13]) and another one from the Aegean Thasos Island (Skala Marion Cave [45]). Additional records are from the northern (Sofular Cave [34] and southern margins of Anatolia (Dim Cave [46]). The Carpathian karst regions is relatively better represented with records from Ceremosnja- [30], Ascunsă- [47], and Ursilor caves [31] and two records from Baradla Cave [18]. There are three entities from the relatively small karstic area in the Southern Transdanubia, the Mecsek Hills, two from the Abaliget- [48] and one from the Trió Cave [11,14].

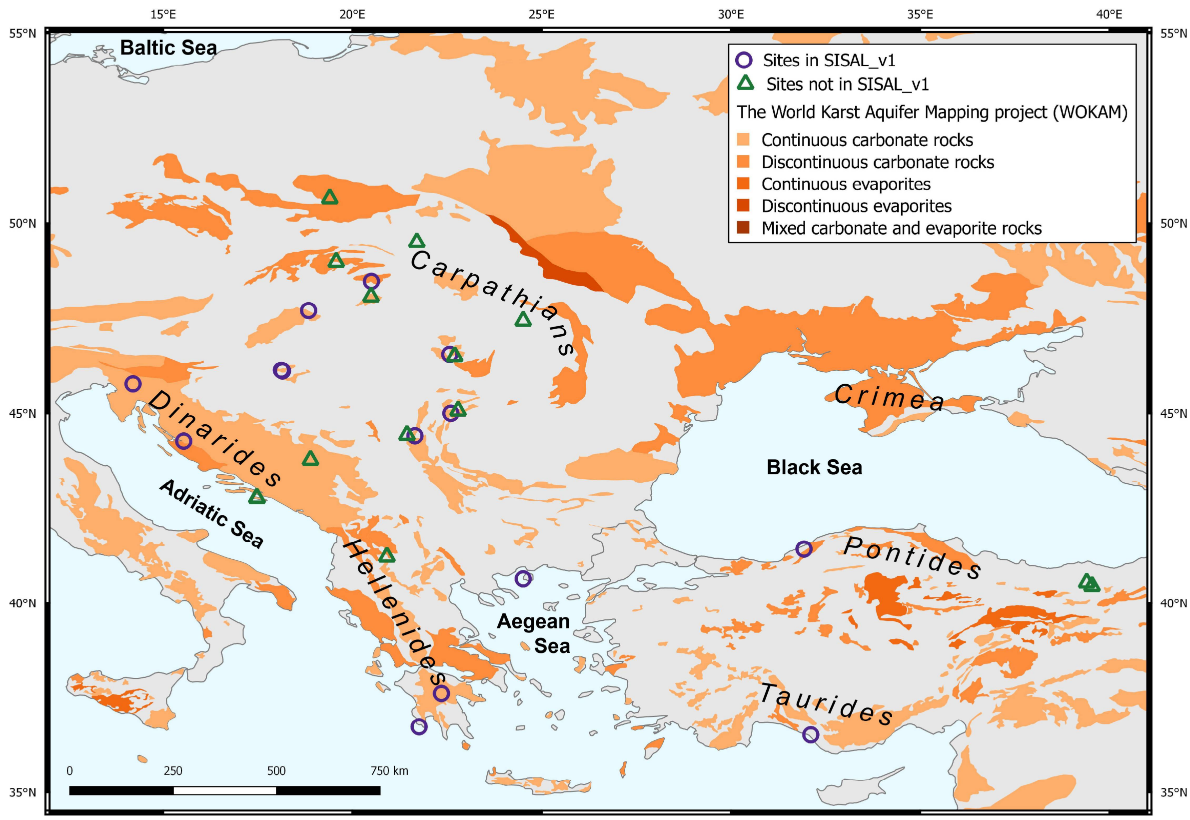

Figure 1. Map indicating the location of speleothem records included in the SISAL v1 and others not yet in the database from Eastern Europe & Turkey showing the karst aquifers (data provided by The World Karts Aquifer Mapping Project [49])

The relative data scarcity in the mid-Balkans (Figure 1) could be reduced since studies have been recently published from Macedonia [50], Croatia [51] and Bosnia [52] (Table 1). Recently published records from Demänovska Valley [53]; Closani Cave [10]; Tausoare and Ascunca caves [54] are also expected to expand the data coverage for the Carpathian region.

There are karst regions in the northern part of the studied area (Figure 1), but only a few speleothem stable isotope records have been identified e.g. [23,55]. One explanation for this is that the permafrost conditions which existed around [56] and beneath the former Fennoscandian Ice Sheet which covered this area [57] very likely prevented speleothem formation (see also [23])

 doi:10.20944/preprints201812.0038.v1

because there was no water movement in the frozen ground. This hypothesis is indirectly supported by a recent study showing flowstone deposition in the Kraków-Częstochowa Upland at 975-470 ka [58]), predating the major glaciations of the region. The thawing of this frozen ground could be a prolonged process after deglaciation [57,59], maintaining unfavorable conditions for speleothem formation. Moreover, the flat terrain means that the current karstwater table is near to the surface, which does not favor subaerial speleothem formation in the sub-terrain cavities.

Additional identified records (Table 1) e.g. from the Romanian Carpathians [32,33] the Low Tatras [60] or the Pontides [20,61,62] may help in increasing the spatiotemporal coverage of the region. These records were not included to the SISAL database yet, either due to difficulties in obtaining data developed and published decade(s) ago or because they did not met SISAL quality criteria [37]. For example, although a single radiometric age broadly constrains the beginning of speleothem formation from Slowianska Drwali Cave (southern Poland) to 12±6 ka [55], it is insufficient to achieve an age-distance model to assign ages to the small set of randomly collected isotope measurements made on the speleothem, rendering this record unsuitable for the SISAL database (Table 1).

Table 1. Metadata of the speleothem records of the Eastern Europe & Turkey SISAL region, included in the SISAL v1 database [37] and records identified but not yet included. Column headings in italics represent field names that can be queried in the SISAL database. Min/Max year the date corresponding to the ultimate/first stable isotope data of the entity respectively. Entities without an entity_id are not in SISAL_v1.

site_name	*site_id*	**Country**	*latitude (N)*	*longitude (E)*	*elevation m amsl*	*entity_name*	*entity_id*	**Min. Year (BP)**	**Max. Year (BP)**	**Reference**
Abaliget Cave	31	Hungary	46.13	18.12	209	ABA_1	105	123303	143456	[48]
						ABA_2	106	140274	160598	[48]
Ascunsă Cave	72	Romania	45.00	22.60	1050	POM2	161	-32	8169	[47]
Baradla Cave	71	Hungary	48.47	20.50	375	BAR-II#B	160	108758	128125	[63]
						BAR-II#L	159	109194	129003	
Ceremosnja Cave	76	Serbia	44.40	21.65	530	CC-1	165	-48	2426	[30]
Dim Cave	79	Turkey	36.53	32.11	232	Dim-E2	168	9738	13094	[46]
						Dim-E3	169	12575	89714	
						Dim-E4	170	12020	14555	
Kapsia Cave	44	Greece	37.62	22.35	700	GK-09-02	120	1115	2904	[13]
Leány Cave	84	Hungary	47.70	18.84	420	Leany	177	4739	10543	[21]
Mavri Trypa Cave	156	Greece	36.74	21.76	70	S1	347	1296	4687	[44]
Modrič Cave	86	Croatia	44.26	15.54	32	MOD-22	179	-58	1637	[43]
Postojna Cave	88	Croatia	45.77	14.20	529	POS-STM-4	181	-46	8	[24]

Preprints (www.preprints.org) | NOT PEER-REVIEWED | Posted: 4 December 2018 doi:10.20944/preprints201812.0038.v1

Skala Marion Cave	56	Greece	40.64	24.51	41	MAR_L	136	1481	5534	[45]
Sofular Cave	141	Turkey	41.42	31.93	700	So-1	305	-56	50275	[34]
Trió Cave	90	Hungary	46.11	18.15	275	Trio	183	3028	4711	[11]
Ursilor Cave	91	Romania	46.55	22.57	482	PU-2	184	-50	7068	[31]
Akcakale Cave		Turkey	40.45	39.54		2p				[61]
Ascunsă cave	72	Romania	45.00	22.60	1050	POM1				[54]
Baradla Cave	71	Hungary	48.47	20.50	375	NU2				[63]
Cloşani Cave		Romania	45.07	22.79	433	C09-2				[10]
						C-6				[64]
Demänovská Cave of Liberty		Slovakia	48.98	19.57		HcH2A, HcH2B				[53]
Demianova Cave System		Slovakia	48.98	19.57		JS7, JMr 14				[60]
Jaskyňa Slowianska Drwali cave		Poland	49.50	21.70	420	sample 2				[55]
Karaca Cave		Turkey	40.54	39.40	1536	K1				[20]
Kiskőhát Shaft		Hungary	48.07	20.49	915	Kiskőhát				[65]
Mala Spilja Cave		Croatia	42.76	17.48	60	MSM-1				[51]
Mračna Cave		Bosnia and Herzegovina	43.77	18.89	597	BS14, BS15				[52]
		Macedonia	41.22	20.91	1130	OH2				[50]
Poleva Cave		Romania	44.42	21.44	390	PP-10				[33]
Sofular Cave	141	Turkey	41.42	31.93	700	SO-2				[34]
						SO-17				[62]
Tauşoare Cave		Romania	47.43	24.51	950	T-1152				[54]
Velika Spilja Cave		Croatia	42.77	17.47	90	VSM-1				[51]
V11 Cave		Romania	46.50	22.70	1254	S139				[66]
						S22, S117				[32]
Wierna Cave		Poland	50.65	19.40	385	JWi2				[23]

* minimum and maximum date of the stable isotope record were rounded to integer

From a temporal perspective, the oldest record in the region is the ABA_2 entity from the Abaliget Cave (Figure 2; Table 1). The period from ~108.8to–~ 160.6 ka is represented by only four

Preprints (www.preprints.org) | NOT PEER-REVIEWED | Posted: 4 December 2018 doi:10.20944/preprints201812.0038.v1

records with two overlapping segments. The first overlap can be seen between the Abaliget records from ~140.2 ka to 143.5 ka and the second one between Baradla records and ABA_1 from ~123.3 ka to 129 ka. This is followed by a cca. 20-kyr-long hiatus up to ~89.7ka (Figure 2). This period is only scarcely represented in certain part of the region [67], although radiometric ages from a couple of speleothems have been reported from this period from the Carpathian karstic regions (e.g. [68,69]). Moreover, a recent compilation of radiometric ages from more than 90 speleothems and flowstones from the Croatian karst show an even temporal distribution back to the onset of MIS5 [7], suggesting there is a good opportunity to develop speleothem stable isotope records for this period.

From ~90 ka onwards, there is continuous coverage for both $\delta^{18}O$ and $\delta^{13}C$ for the records from Eastern Europe & Turkey, although most of the period is characterized by low replication of records. The Dim-E3 record stretches from 89.7 ka to 12.6 ka overlapping with the So-1 record from 50.3 ka (Table 1). These two speleothems are the only records from the region until 10.5ka when the Leany record starts (Figure 3).

The Holocene is the best represented period in the region (Figure 2, 3, 4). The period from ~1.42 ka to ~2.05 ka with its 7 records is the most represented in the region: PU-2, GK-09-02, MAR_L, POM2, CC-1, So-1 and S1. Before this date, a coinciding hiatus characterizes the time series of the Ursilor- and Skala Marion Cave entities; from ~2.2 ka to ~3 ka, which may suggest a sub-regional pattern with conditions unfavorable for speleothem formation.

There is a good chance to further extend the regional dataset beyond the MIS6, since entities predating the current dataset have already been identified from Turkish [62], Macedonian [50], Croatian [70] and Hungarian [71] localities. Moreover, calcareous cave deposits exceeding the current limit of applicability of U-Th dating method can be found in the region [58].

 doi:10.20944/preprints201812.0038.v1

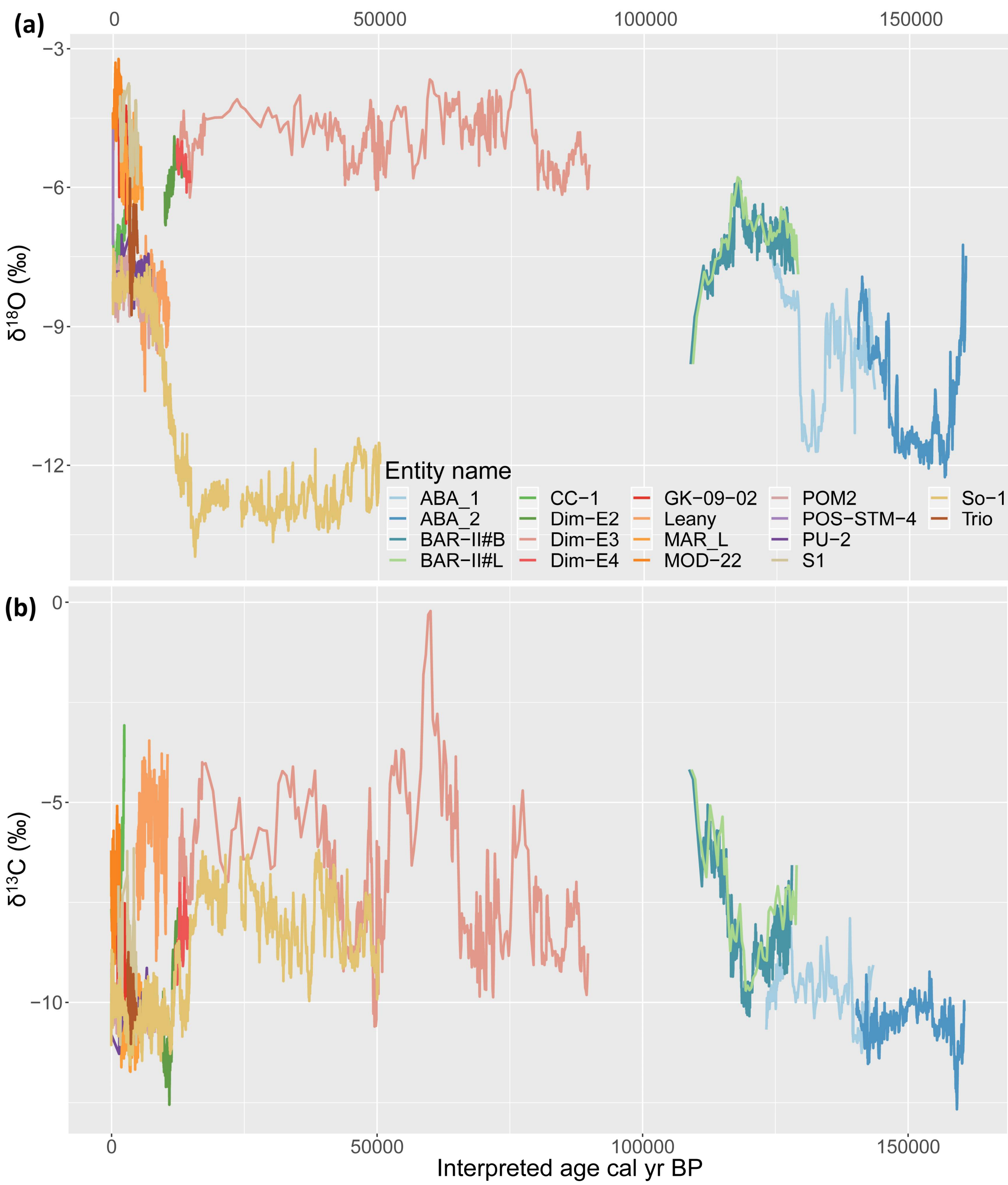

Figure 2. Temporal span of individual speleothem records in the Eastern Europe & Turkey SISAL region for (a) $\delta^{18}O$ and (b) $\delta^{13}C$ for the last 160 ka

The average length of the records is ~13.8ka and the median is 4.9ka, including hiatuses. The shortest growth period was 54yrs (POS-STM-4), the longest spanned ~77.1ka (Dim-E3). The temporal resolution of the SISAL archived speleothem stable isotope records of the Eastern Europe & Turkey region ranges from sub-decadal (So-1, [34], S1 [44]; Trió, [11] to >1000yr (Dim-E3, [46]). The characteristic temporal resolution of the available speleothem stable isotope records can be estimated to 12 yr for the Holocene, while it is usually >50 yr for the pre-Holocene period (Figure 3). The studies following the pioneering record of PU-2 [31], achieved characteristically finer temporal resolution (Figure 3).

 doi:10.20944/preprints201812.0038.v1

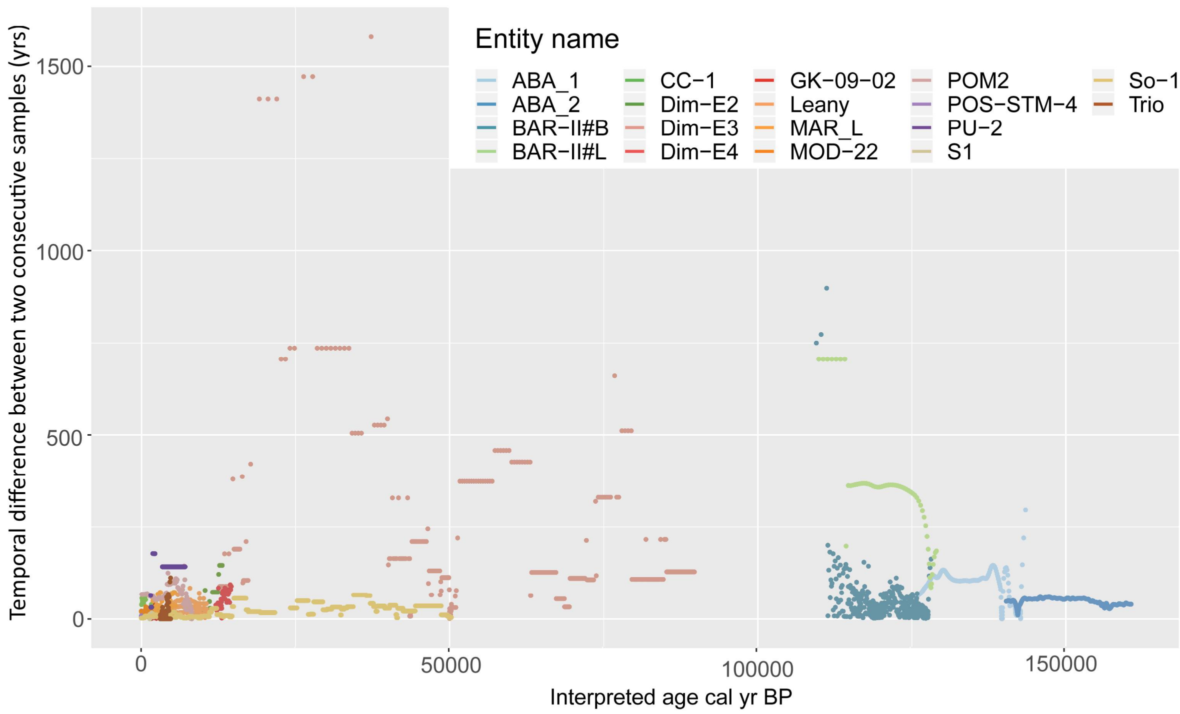

Figure. 3. Temporal difference between two consecutive samples for the Eastern Europe & Turkey SISAL region's records.

3.2 Environmental controls on stable isotope composition of speleothem carbonate

Out of the 14 cave systems studied in the Eastern Europe & Turkey SISAL region (8.6% of the total number in the SISAL_v1 database [37]), 7 have been monitored.

Monitoring of key variables (e.g. cave temperature, ventilation) regulating dripwater hydrology and saturation conditions in caves provides a basis for the process-based understanding of environmental controls on stable isotope composition of speleothem carbonate and speleothem growth conditions at specific cave-settings (e.g. [72,73]). A weakness of the early period of speleothem-based paleoscience in the region is the previously presented relatively modest level of monitoring. Consequently, in the lack of site-specific information (site specific infiltration processes, calcite precipitation), most of the paleoclimatic inferences of these studies relied on general notions. However, recently this knowledge-gap began to be filled by speleological monitoring studies becoming abundant in the region [10,74-80]. This predicts that much more experimental experience is being made available to help the interpretation of the speleothem recorded geochemical signatures over the region in the forthcoming studies.

Thorough monitoring enabled a recent study to compare modeled and measured dripwater $\delta^{18}O$ in Postojna Cave [81]. Monthly measured precipitation (amount and $\delta^{18}O$) and ratio of evapotranspiration were the input parameters, while the mixing and delay process taking place during infiltration were statistically simulated in the model. There was excellent agreement between the measured $\delta^{18}O_{spel}$ and the modeled ones calculated using the modeled dripwater $\delta^{18}O$ between 1984 and 2002. Such studies are to become more-and-more abundant as cave monitoring advances, thus providing an improved process-based understanding for the interpretation of speleothem archived isotope geochemical signatures.

3.2.1 Environmental controls on speleothem $\delta^{18}O$

Paleoclimatic interpretation of speleothem $\delta^{18}O$ variations requires knowledge and quantitative estimation of processes that may affect the isotopic composition of water during the course of the

 doi:10.20944/preprints201812.0038.v1

hydrologic cycle and during calcite deposition. For a general introduction to environmental controls on speleothem $\delta^{18}O$ the reader is referred to (LEAD PAPER to be cited).

The stable isotope composition of precipitation correlates positively with temperature in the Eastern Europe & Turkey SISAL region [82-84] as generally seen in the extratropics [85].

A progressively stronger correlation between the water stable isotope content of monthly precipitation and local surface air temperature was registered moving inland across Europe [86]. A related pattern is seen dividing the warm Mediterranean coastal sites and the continental ones regarding the modern day $\delta^{18}O$/T slope (so-called "temperature effect") (Figure 5). The temperature effect ranges from ~0.15‰ per °C for coastal sites (e.g. Figure 4, [87]) to ~0.35‰ per °C for most continental locations (e.g. Figure 5, [84]).

In the coastal regions the modern day $\delta^{18}O$/T slope is below the water-calcite isotopic equilibrium fractionation factor (−0.24‰ °C−1 [88]), while in the more continental locations it is above it (Figure).

This is an important split; it explains a major part why the oxygen isotope composition of more continental formations is thought to reflect mainly temperature variation and changes in moisture transport trajectories transferred via source water $\delta^{18}O$ fluctuation, while $\delta^{18}O_{spel}$ strongly reflects fluctuations of precipitation amount in the southern part of the region. The correspondence, for instance, between the interannual variability of total amount of late autumn–winter precipitation (October to January) and $\delta^{18}O_{spel}$ from Akcacale Cave (not yet in the database Table 1) is sufficiently strong to permit to achieve the first quantitative reconstruction of October to January precipitation [61,89].

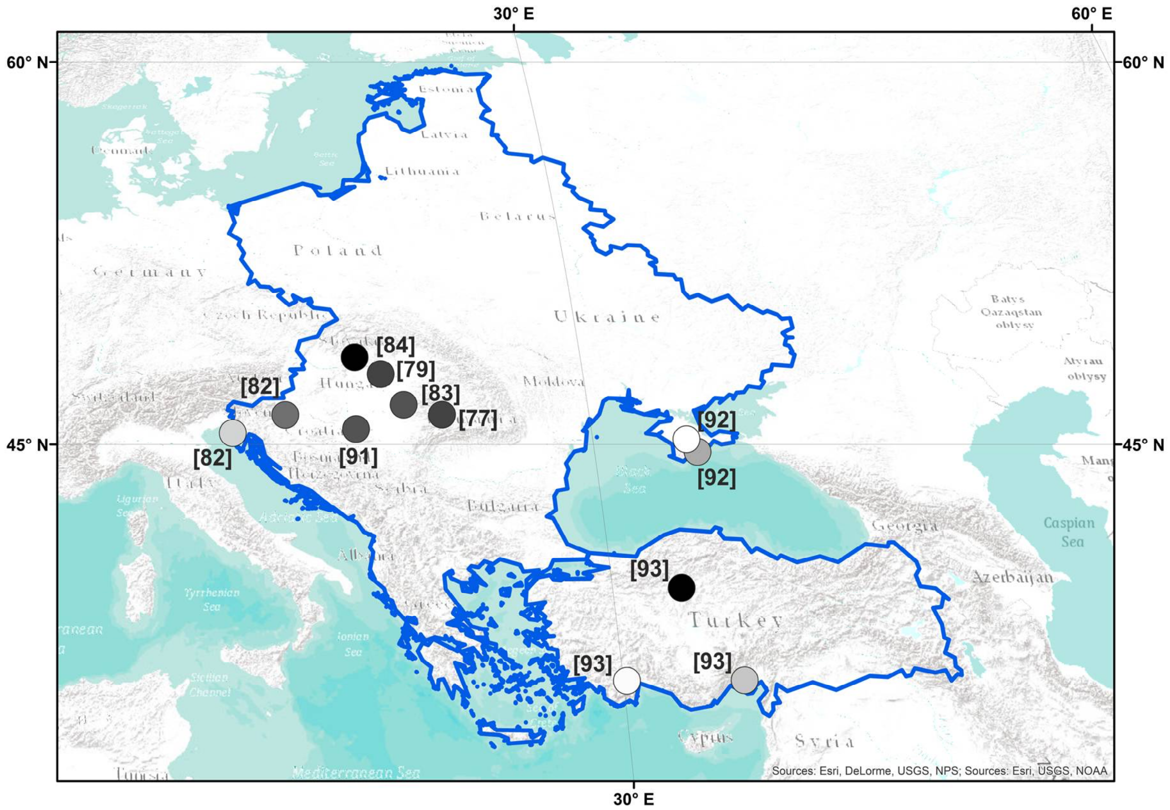

Figure 4. Map of the Eastern Europe & Turkey SISAL region, with the modern day $\delta^{18}O$/T slopes indicated by circles shaded in greyscale proportionate to the slope (min 0.16‰/°C: white; max 0.36‰/°C: black). The numbers in brackets next to the circles indicate the references for the corresponding studies; Slovenia: [82,90], Serbia: [91], Hungary: [79,83], Slovakia: [84], Romania: [77], Crimea: [92], Turkey: [93].

 doi:10.20944/preprints201812.0038.v1

3.2.2 Environmental controls on speleothem δ^{13}C

For a general introduction to environmental controls on speleothem δ^{18}O the reader is referred to (LEAD PAPER to be cited). Variations of δ^{13}C primarily interpreted by changes in paleohydrology, such as soil biological activity (Abaliget Cave [48], Ascunsă Cave [47], Baradla Cave [63]Trio Cave [11], Skala Marion Cave [45], Mavri Trypa Cave [44], Kapsia Cave [13] related to humidity changes or simplified to corresponding low/high δ^{13}C values with dry/wet periods (Ursilor Cave [31], Modrič Cave [43]. For instance, P contents of the Trió speleothem supported that the δ^{13}C values reflect humidity-related changes in soil biological activity [11].

In Anatolian karst representing warm semi-arid environments, the secular changes in δ^{13}C may track changes in the dominance of C3 vs C4 in the vegetation type (Dim Cave [46], Sofular Cave [34]).

The relatively enriched (δ^{13}C > -5‰) carbon isotope compositions identified in Dim Cave and Leány caves (Figure 2) supposedly occurred due to changes in ventilation effect [21,46]. This degassing related kinetic fractionation cause an increase of the δ^{13}C value partly overprinting the paleohydrological signals, although, minima in speleothem δ^{13}C curves can be regarded as largely unaffected by such kinetic processes [48].

4. Regional patterns in oxygen and carbon isotope records through time

Conventionally stalagmite formation in isotopic equilibrium is assessed on the base of weak or no correlation between speleothem δ^{13}C and δ^{18}O values measured along the growth axis as well as along the same growth lamina (Hendy, 1971). The lack of significant correlation between the C and O isotope compositions suggests quasi-equilibrium, carbonate precipitation can be assumed with a minor kinetic effect in the case of the ABA_1 (p=0.044), PU-2 (p=0.251) Dim-E4 (p=0.089) entities (Figure S2, Table S1).

The highest positive slope (2.64) with a significant correlation (adj. R^2=0.45; p<6.5E-15) between δ^{13}C and δ^{18}O was observed in the CC-1 record. However, this is because the samples were gathered along a radial transect [30], rather than along the growth axis of the entity so that the kinetic effect is exaggerated as sampling points getting closer to the edge. The strongest correlation (adj. R^2=0.64) although with a less steep slope of 0.35 (p<0.003) is seen in the short dataset of Pos-STM-4 record (Figure S2, Table S1). The kinetic effect was not an issue in the original study, because its primary scope was the detection of the ^{14}C activity increase due to nuclear tests in the atmosphere and modeling the dynamics of soil carbon pools producing soil CO_2 [24]. However, this has to be considered when querying the database for entries applicable in (paleo)climatological studies. In addition, in the Dim-E2, E3 and S1 records, δ^{13}C also had a positive significant (p<1.7E-15) slope (>1.4) with δ^{18}O. In such cases, major kinetic effect can be expected to have occurred during carbonate precipitation.

A weak correlation between δ^{18}O and δ^{13}C values is not a prerequisite of isotopic equilibrium; however, the replication test (i.e., a high degree of coherence between individual δ^{18}O and/or δ^{13}C profiles from different speleothems from the same cave over the common time period) is a more stringent test of isotopic equilibrium [94].

The SISAL database can provide the basis for *regional* replication tests. The pronounced enrichment signal expressed in the δ^{13}C values prevailing in the older section of the CC-1 record and preceding the growth stops of S1 records is hardly replicated in the coeval records from the region (Figure S3b). This suggests that at least some sections of these records (e.g. S1) carry a strong kinetic effect and should be treated with caution.

4.1. Assessment of spatial patterns in the Holocene

The SISAL_v1 database contains 12 records from the past 11.6 kyr from Eastern Europe and Turkey. In the mid-Holocene, the relatively higher abundance of data (Figure S3a) provided a

Preprints (www.preprints.org) | NOT PEER-REVIEWED | Posted: 4 December 2018 doi:10.20944/preprints201812.0038.v1

glimpse on the spatial tendencies of $\delta^{18}O_{spel}$. The average $\delta^{18}O_{spel}$ was calculated for contemporarily formed deposits from three separate semi-millennial periods from the Holocene. Unlike previous observations [95] latitudinal or continental trends could not be observed probably due to the limited spatial extent of the region (latitudinal extent <10°, longitudinal extent <12°). However, there are negative correlations between $\delta^{18}O$ records from eastern and southeastern Europe and elevation, even though "site elevation" in the database [37] corresponds to the cave entrance rather than the elevation of recharge of dripwater (Figure 5). It can be assumed that the difference in site elevation is likely to properly reflect the difference in infiltration area elevations. Despite this uncertainty regarding the elevation of the actual recharge area, estimated $\delta^{18}O_{spel}$ elevation gradients calculated for three non-overlapping semi-centennial periods (and excluding records with high risk of kinetic effects) during the past ~5 kyr suggests that this elevation trend is characteristic of the Holocene. Computed elevation gradients were significant (at $p<0.1$ level) in all but one cases and ranged between -0.25(±0.11) ‰/100m and -0.27(±0.08) ‰/100m.

Isotopic depletion of meteoric precipitation with elevation is expected [96] and has been measure in this region as ranging from -0.24 ‰/100m to -0.39 ‰/100m [73,87,97,98]. Slightly flatter elevation gradients are reported both for isotopic composition of (i) shallow groundwater (-0.24 ‰/100m, [99], interquartile interval: from -0.11 to -0.24 ‰/100m, [100] and (ii) dripwater (-0.11‰/100m, [73]).

Although it might be expected that the speleothem-derived gradient would be closer to that of shallow groundwater and of dripwater; interestingly, it in fact resembles that of precipitation most closely. Testing whether the found $\delta^{18}O_{spel}$ gradient is prevailing over geological timescales especially under distinct climate settings, such as the LGM can be achieved with an increased entity numbers providing a much improved replication in this specific period. The robustness of this empirical $\delta^{18}O_{spel}$ gradient can be further explored extending the region of towards nearby SISAL regions, e.g. [101].

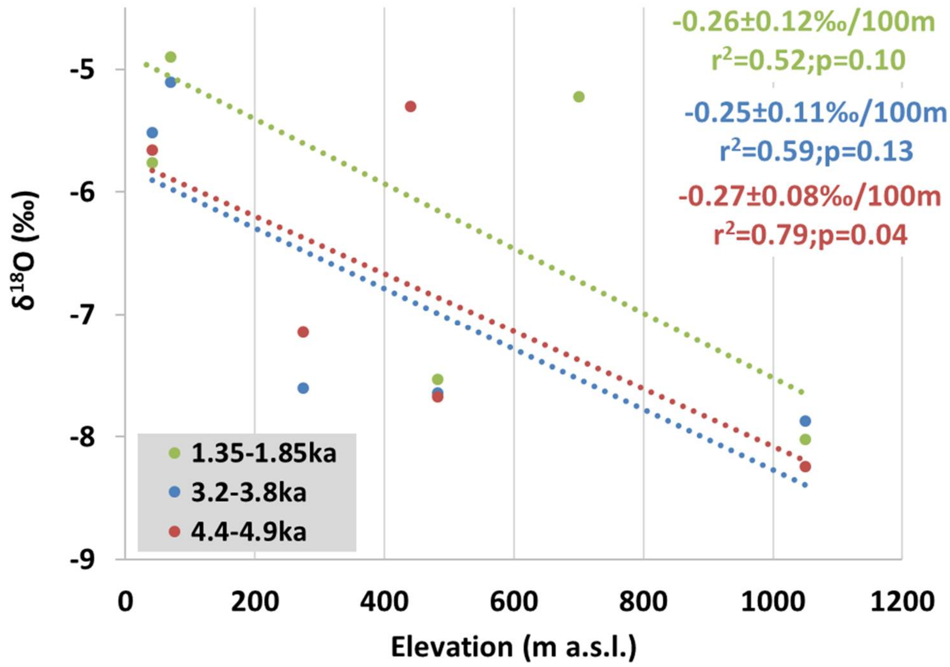

Figure. 5. Elevation gradient of $\delta^{18}O_{spel}$ for three semi-millennial time horizons for the past 5000 yrs for SE Europe

 doi:10.20944/preprints201812.0038.v1

4.2 Cryogenic cave carbonates, special calcareous speleothems from the region

Coarsely crystalline cryogenic cave carbonates (CCCcoarse) from Central Europe represent a novel archive to study the extent of permafrost in the past (e.g. [102-105] CCCcoarse deposits are formed because permafrost thawing allows water starts to percolate through the epikarst and penetrate into the still-frozen cave system where it slowly freezes, becoming increasingly enriched in ions until the solution is supersaturated and carbonate precipitates [102]. Cryogenic carbonate has a very specific isotope composition [105,106].

CCCcoarse have been described in several caves in Europe [105] including karst areas from the Eastern Europe part of this SISAL region (Poland and Slovakia; [102,104,105,107]). U-Th dating of cryogenic minerals from the Last Glacial period typically suggest that most of the CCCcoarse deposits were formed between ~40 to 21ka BP, indicating the presence of a widespread permafrost zone extending beyond the southernmost limit of the Fennoscandian Ice Sheet [105].

There are seven peaks in the temporal distribution of the sum probability of CCCcoarse occurrences over the past 40 kyrs (Figure 6). Some of these peaks (at ~12, ~16, ~25 and ~36ka) correspond to regional minima of $\delta^{18}O_{spel}$ (So-1 and Dim-E4 records; Figure 6a), though these speleothems are from Anatolia. 6The CCCcoarse occurrences at ~12 and ~25ka correspond with regional minima of annual mean temperature inferred from branched glycerol dialkyl glycerol tetraethers (brGDGT; Figure 6b) from speleothems in the same region However, there is no correspondence between interstadial transitions in the NorthGRIP ice core $\delta^{18}O$ record [108] and CCCcoarse occurrences (Figure 6d) nor do the other CCCcoarse occurrences match $\delta^{18}O_{spel}$ or brGDGT-inferred temperature minima. Thus our regional assessment does not appear to confirm the hypothesis that the temporal distribution of CCCcoarse occurrences coincide with transitions from stadial to interstadial conditions [105], which otherwise is thought to be in agreement with the published model of CCCcoarse formation in ice filled cavities within the permafrost [103].

Linking the maxima of CCCcoarse occurrences and the minima of the regional paleotemperature proxies (Fig. 6) is a logical and straightforward interpretation, as viable as their formation explained with the thawing of the permafrost layer above the cavities [103]. The correspondence of CCCcoarse occurrence peak with locally more relevant temperature reconstructions could be scrutinized also in other SISAL regions, where radiometric ages for CCCcoarse occurrences are available.

Preprints (www.preprints.org) | NOT PEER-REVIEWED | Posted: 4 December 2018 doi:10.20944/preprints201812.0038.v1

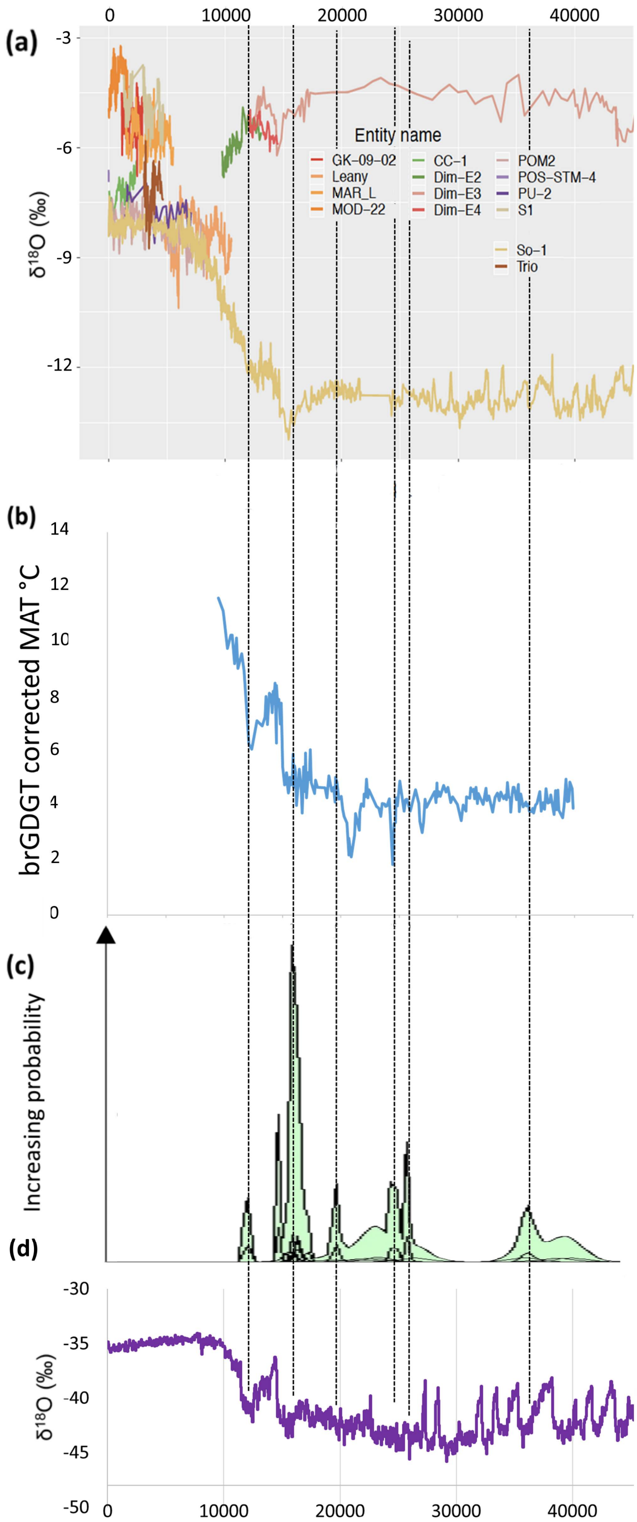

Figure 6. Time series of (a) $\delta^{18}O$ speleothem records in the Eastern Europe & Turkey SISAL region, (b) annual mean temperature inferred from branched glycerol dialkyl glycerol tetraethers (brGDGT) calibrated with a global training set - MD04-2790 Black Sea core - (redrawn from [109]) and (c) probability distribution plot [110] of U-Th ages of coarsely crystalline cave carbonate from the Eastern Europe [102,105,107] and (d) 50-yr averaged $\delta^{18}O$ of the Greenland Ice Sheet (NorthGRIP ice core) [108] relative to V-SMOW for the last 45,000 yrs. The black vertical dotted lines indicate the coincidence of the probability peaks of the sum density functions, to the speleothem and ice core $\delta^{18}O$ records, and the regional mean annual temperature reconstruction.

 doi:10.20944/preprints201812.0038.v1

5. Conclusions and outlook

There are comparatively few records from Eastern Europe and Turkey in the SISAL database, and most of these records only cover the Holocene. The Sofular Cave So-1 entity is the sole record in SISAL_v1 covering glacial cycles and extending back the Holocene. Thus, there is a strong need to gather such speleothems, since these provide a continuous record of the environmental response induced by a transition from cold glacial to warm interglacial climate regime.

Nevertheless, the diverse karst landscape of Eastern Europe & Turkey offer a great potential for reconstructing past environmental changes based on isotope records from speleothems. There is potential to expand the database by including recently published material, and exploration and exploitation of regions such as the Dinaric Karst [7] will yield more data in the near future.

The SISAL database can provide a solid basis for regional replication tests pointing out regionally incoherent variations from individual $\delta^{18}O$ and/or $\delta^{13}C$ profiles.

The regional subset, does not appear to confirm the existence of longitudinal trends in $\delta^{18}O_{spel}$ across Eastern Europe during the Holocene. This likely reflects the relatively short distances involved. The existence of the SISAL database provides an opportunity to go beyond regional data syntheses to examine spatial patterns at a much larger scale [101]. Spatial scale is not an issue for the examination of elevation gradients, and here the data from Eastern Europe provide clear-cut evidence for elevational gradients in $\delta^{18}O_{spe}$ during the Holocene (-0.26‰ 100m^{-1}). Comparative studies from other regions could provide insights into the stability of these gradients through time.

Funding: This research was funded by the Hungarian Academy of Sciences (MTA "Lendület" program; LP2012-27/2012) and the János Bolyai Research Scholarship of the Hungarian Academy of Sciences.

Acknowledgments

Authors thank all colleagues involved in SISAL for intriguing discussions and collaboration on the preparation of this manuscript. SISAL is a working group of the Past Global Changes (PAGES) programme and we thank PAGES for their support of this activity. We are grateful to Sandy Harrison and Laia Comas Bru for detailed and constructive criticism and editorial handling of the manuscript. Authors also thank the members of the World Karst Aquifer Mapping project for providing the shape file used to derive the carbonate aquifer maps (Figure 2).

Conflicts of Interest: The authors declare no conflict of interest. The funders had no role in the design of the study; in the collection, analyses, or interpretation of data; in the writing of the manuscript, or in the decision to publish the results.

Preprints (www.preprints.org) | NOT PEER-REVIEWED | Posted: 4 December 2018 doi:10.20944/preprints201812.0038.v1

References

1. Cvijić, J. *Das karstphänomen: Versuch einer morphologischen monographie.* Hölzel: 1893.
2. Cvijic, J. Hydrographie souterraine et évolution morphologique du karst. *Revue de Géographie Alpine* **1918**, *6*, 375-426.
3. von Terzaghi, C. *Beitrag zur hydrographie und morphologie des kroatischen karstes.* Buchdruckerei des Franklin-vereins: Budapest, 1913.
4. Gabrovšek, F. 60 years of karst research institute zrc sazu: The insider's story of who is who at the karst research institute. *Acta Carsologica* **2007**, *36*.
5. Racoviţă, G. The founder of biospeleology and world's first speleological institute. In *Cave and karst systems of romania*, Ponta, G.M.L.; Onac, B.P., Eds. Springer International Publishing: Cham, 2019; pp 1-3.
6. Surić, M. Submarine karst of croatia-evidence of former lower sea levels. *Acta Carsologica* **2002**, *31*, 89-98.
7. Surić, M. Speleothem-based quaternary research in croatian karst – a review. *Quaternary International* **2018**, *490*, 113-122.
8. Nita, D.; Richards, D.; Surić, M.; De Waele, J. In *Mc-icpms u-th age determinations on altered submerged speleothems from croatia*, NSF Workshop" Sea-level Changes into MIS 5: from observations to prediction", 2012.
9. Surić, M.; Richards, D.A.; Hoffmann, D.L.; Tibljaš, D.; Juračić, M. Sea-level change during mis 5a based on submerged speleothems from the eastern adriatic sea (croatia). *Marine Geology* **2009**, *262*, 62-67.
10. Warken, S.F.; Fohlmeister, J.; Schröder-Ritzrau, A.; Constantin, S.; Spötl, C.; Gerdes, A.; Esper, J.; Frank, N.; Arps, J.; Terente, M.*, et al.* Reconstruction of late holocene autumn/winter precipitation variability in sw romania from a high-resolution speleothem trace element record. *Earth and Planetary Science Letters* **2018**, *499*, 122-133.
11. Demény, A.; Kern, Z.; Czuppon, G.; Németh, A.; Schöll-Barna, G.; Siklósy, Z.; Leél-Őssy, S.; Cook, G.; Serlegi, G.; Bajnóczi, B.*, et al.* Middle bronze age humidity and temperature variations, and societal changes in east-central europe. *Quaternary International* **2018**.
12. Ünal-İmer, E.; Shulmeister, J.; Zhao, J.-X.; Uysal, I.T.; Feng, Y.-X. High-resolution trace element and stable/radiogenic isotope profiles of late pleistocene to holocene speleothems from dim cave, sw turkey. *Palaeogeography, Palaeoclimatology, Palaeoecology* **2016**, *452*, 68-79.
13. Finné, M.; Bar-Matthews, M.; Holmgren, K.; Sundqvist, H.S.; Liakopoulos, I.; Zhang, Q. Speleothem evidence for late holocene climate variability and floods in southern greece. *Quaternary Research* **2014**, *81*, 213-227.
14. Siklósy, Z.; Demény, A.; Vennemann, T.W.; Pilet, S.; Kramers, J.; Leél-Őssy, S.; Bondár, M.; Shen, C.-C.; Hegner, E. Bronze age volcanic event recorded in stalagmites by combined isotope and trace element studies. *Rapid Communications in Mass Spectrometry* **2009**, *23*, 801-808.

 doi:10.20944/preprints201812.0038.v1

15. Siklosy, Z.; Kern, Z.; Demeny, A.; Pilet, S.; Leel-Ossy, S.; Lin, K.; Shen, C.-C.; Szeles, E.; Breitner, D. Speleothems and pine trees as sensitive indicators of environmental pollution – a case study of the effect of uranium-ore mining in hungary. *Applied Geochemistry* **2011**, *26*, 666-678.
16. Badertscher, S.; Borsato, A.; Frisia, S.; Cheng, H.; Edwards, R.L.; Tüysüz, O.; Fleitmann, D. Speleothems as sensitive recorders of volcanic eruptions – the bronze age minoan eruption recorded in a stalagmite from turkey. *Earth and Planetary Science Letters* **2014**, *392*, 58-66.
17. McDermott, F. Palaeo-climate reconstruction from stable isotope variations in speleothems: A review. *Quaternary Science Reviews* **2004**, *23*, 901-918.
18. Demény, A.; Kern, Z.; Czuppon, G.; Németh, A.; Leél-Őssy, S.; Siklósy, Z.; Lin, K.; Hu, H.-M.; Shen, C.-C.; Vennemann, T.W.*, et al.* Stable isotope compositions of speleothems from the last interglacial – spatial patterns of climate fluctuations in europe. *Quaternary Science Reviews* **2017**, *161*, 68-80.
19. Demény, A.; Siklósy, Z. Combination of off-line preparation and continuous flow mass spectrometry: D/h analyses of inclusion waters. *Rapid Communications in Mass Spectrometry* **2008**, *22*, 1329-1334.
20. Rowe, P.J.; Mason, J.E.; Andrews, J.E.; Marca, A.D.; Thomas, L.; van Calsteren, P.; Jex, C.N.; Vonhof, H.B.; Al-Omari, S. Speleothem isotopic evidence of winter rainfall variability in northeast turkey between 77 and 6 ka. *Quaternary Science Reviews* **2012**, *45*, 60-72.
21. Demény, A.; Czuppon, G.; Siklósy, Z.; Leél-Őssy, S.; Lin, K.; Shen, C.-C.; Gulyás, K. Mid-holocene climate conditions and moisture source variations based on stable h, c and o isotope compositions of speleothems in hungary. *Quaternary International* **2013**, *293*, 150-156.
22. Demény, A.; Czuppon, G.; Kern, Z.; Leél-Őssy, S.; Németh, A.; Szabó, M.; Tóth, M.; Wu, C.-C.; Shen, C.-C.; Molnár, M.*, et al.* Recrystallization-induced oxygen isotope changes in inclusion-hosted water of speleothems – paleoclimatological implications. *Quaternary International* **2016**, *415*, 25-32.
23. Pazdur, A.; Pazdur, M.F.; Pawlyta, J.; Górny, A.; Olszewski, M. Paleoclimatic implications of radiocarbon dating of speleothems from the cracow-wieluń upland, southern poland. *Radiocarbon* **1995**, *37*, 103-110.
24. Genty, D.; Vokal, B.; Obelic, B.; Massault, M. Bomb 14c time history recorded in two modern stalagmites — importance for soil organic matter dynamics and bomb 14c distribution over continents. *Earth and Planetary Science Letters* **1998**, *160*, 795-809.
25. Perşoiu, A.; Onac, B.P.; Wynn, J.G.; Blaauw, M.; Ionita, M.; Hansson, M. Holocene winter climate variability in central and eastern europe. *Scientific Reports* **2017**, *7*, 1196.
26. Kern, Z.; Bočić, N.; Sipos, G. Radiocarbon dated vegetal remains from the cave ice deposits of velebit mt., croatia. *Radiocarbon* **2018**, *In press*.
27. Johnston, V.E.; McDermott, F.; Tămaş, T. A radiocarbon dated bat guano deposit from n.W. Romania: Implications for the timing of the little ice age and medieval

climate anomaly. *Palaeogeography, Palaeoclimatology, Palaeoecology* **2010**, *291*, 217-227.
28. Forray, F.L.; Onac, B.P.; Tanţău, I.; Wynn, J.G.; Tămaş, T.; Coroiu, I.; Giurgiu, A.M. A late holocene environmental history of a bat guano deposit from romania: An isotopic, pollen and microcharcoal study. *Quaternary Science Reviews* **2015**, *127*, 141-154.
29. Cleary, D.M.; Onac, B.P.; Tanţău, I.; Forray, F.L.; Wynn, J.G.; Ionita, M.; Tămaş, T. A guano-derived δ13c and δ15n record of climate since the medieval warm period in north-west romania. *Journal of Quaternary Science* **2018**, *33*, 677-688.
30. Kacanski, A.; Carmi, I.; Shemesh, A.; Kronfeld, J.; Yam, R.; Flexer, A. Late holocene climatic change in the balkans: Speleothem isotopic data from serbia. *Radiocarbon* **2001**, *43*, 647-658.
31. Onac, B.P.; Constantin, S.; Lundberg, J.; Lauritzen, S.-E. Isotopic climate record in a holocene stalagmite from ursilor cave (romania). *Journal of Quaternary Science* **2002**, *17*, 319-327.
32. Tămaş, T.; Onac, B.P.; Bojar, A.-V. Lateglacial-middle holocene stable isotope records in two coeval stalagmites from the bihor mountains, nw romania. *Geological Quarterly* **2005**, *49*, 185-194.
33. Constantin, S.; Bojar, A.-V.; Lauritzen, S.-E.; Lundberg, J. Holocene and late pleistocene climate in the sub-mediterranean continental environment: A speleothem record from poleva cave (southern carpathians, romania). *Palaeogeography, Palaeoclimatology, Palaeoecology* **2007**, *243*, 322-338.
34. Fleitmann, D.; Cheng, H.; Badertscher, S.; Edwards, R.L.; Mudelsee, M.; Göktürk, O.M.; Fankhauser, A.; Pickering, R.; Raible, C.C.; Matter, A.*, et al.* Timing and climatic impact of greenland interstadials recorded in stalagmites from northern turkey. *Geophysical Research Letters* **2009**, *36*.
35. Kottek, M.G., Jürgen; Beck, Christoph; Rudolf, Bruno; Rubel, Franz. World map of the köppen-geiger climate classification updated. *Meteorologische Zeitschrift* **2006**, *15*, 259-263.
36. Ciric, D.; Nieto, R.; Losada, L.; Drumond, A.; Gimeno, L. The mediterranean moisture contribution to climatological and extreme monthly continental precipitation. *Water* **2018**, *10*.
37. Atsawawaranunt, K.; Comas-Bru, L.; Amirnezhad Mozhdehi, S.; Deininger, M.; Harrison, S.P.; Baker, A.; Boyd, M.; Kaushal, N.; Ahmad, S.M.; Ait Brahim, Y.*, et al.* The sisal database: A global resource to document oxygen and carbon isotope records from speleothems. *Earth Syst. Sci. Data* **2018**, *10*, 1687-1713.
38. Hartmann, A.; Gleeson, T.; Rosolem, R.; Pianosi, F.; Wada, Y.; Wagener, T. A large-scale simulation model to assess karstic groundwater recharge over europe and the mediterranean. *Geosci. Model Dev.* **2015**, *8*, 1729-1746.
39. Mätlik, O.; Post, P. Synoptic weather types that have caused heavy precipitation in estonia in the period 1961–2005. *Estonian Journal of Engineering* **2008**, *14*, 195-208.

 doi:10.20944/preprints201812.0038.v1

40. Gómez-Hernández, M.; Drumond, A.; Gimeno, L.; Garcia-Herrera, R. Variability of moisture sources in the mediterranean region during the period 1980–2000. *Water Resources Research* **2013**, *49*, 6781-6794.
41. Krklec, K.; Domínguez-Villar, D.; Lojen, S. The impact of moisture sources on the oxygen isotope composition of precipitation at a continental site in central europe. *Journal of Hydrology* **2018**, *561*, 810-821.
42. Göktürk, O.M.; Fleitmann, D.; Badertscher, S.; Cheng, H.; Edwards, R.L.; Leuenberger, M.; Fankhauser, A.; Tüysüz, O.; Kramers, J. Climate on the southern black sea coast during the holocene: Implications from the sofular cave record. *Quaternary Science Reviews* **2011**, *30*, 2433-2445.
43. Rudzka, D.; McDermott, F.; Surić, M. A late holocene climate record in stalagmites from modrič cave (croatia). *Journal of Quaternary Science* **2012**, *27*, 585-596.
44. Finné, M.; Holmgren, K.; Shen, C.-C.; Hu, H.-M.; Boyd, M.; Stocker, S. Late bronze age climate change and the destruction of the mycenaean palace of nestor at pylos. *PLOS ONE* **2017**, *12*, e0189447.
45. Psomiadis, D.; Dotsika, E.; Albanakis, K.; Ghaleb, B.; Hillaire-Marcel, C. Speleothem record of climatic changes in the northern aegean region (greece) from the bronze age to the collapse of the roman empire. *Palaeogeography, Palaeoclimatology, Palaeoecology* **2018**, *489*, 272-283.
46. Ünal-İmer, E.; Shulmeister, J.; Zhao, J.-X.; Tonguç Uysal, I.; Feng, Y.-X.; Duc Nguyen, A.; Yüce, G. An 80 kyr-long continuous speleothem record from dim cave, sw turkey with paleoclimatic implications for the eastern mediterranean. *Scientific Reports* **2015**, *5*, 13560.
47. Drăguşin, V.; Staubwasser, M.; Hoffmann, D.L.; Ersek, V.; Onac, B.P.; Veres, D. Constraining holocene hydrological changes in the carpathian–balkan region using speleothem δ¹⁸o and pollen-based temperature reconstructions. *Clim. Past* **2014**, *10*, 1363-1380.
48. Koltai, G.; Spötl, C.; Shen, C.-C.; Wu, C.-C.; Rao, Z.; Palcsu, L.; Kele, S.; Surányi, G.; Bárány-Kevei, I. A penultimate glacial climate record from southern hungary. *Journal of Quaternary Science* **2017**, *32*, 946-956.
49. Chen, Z.; Auler, A.S.; Bakalowicz, M.; Drew, D.; Griger, F.; Hartmann, J.; Jiang, G.; Moosdorf, N.; Richts, A.; Stevanovic, Z.*, et al.* The world karst aquifer mapping project: Concept, mapping procedure and map of europe. *Hydrogeol J* **2017**, *25*, 771-785.
50. Regattieri, E.; Zanchetta, G.; Isola, I.; Bajo, P.; Perchiazzi, N.; Drysdale, R.N.; Boschi, C.; Hellstrom, J.C.; Francke, A.; Wagner, B. A mis 9/mis 8 speleothem record of hydrological variability from macedonia (f.Y.R.O.M.). *Global and Planetary Change* **2018**, *162*, 39-52.
51. Lončar, N.; Bar-Matthews, M.; Avalon, A.; Surić, M.; Faivre, S. Early and mid-holocene environmental conditions in the eastern adriatic recorded in speleotherms from mala špilja cave and velika špilja cave (mljet island, croatia). *Acta Carsologica* **2017**, *46*, 229-249.

52. Chiarini, V.; Couchoud, I.; Drysdale, R.; Bajo, P.; Milanolo, S.; Frisia, S.; Greig, A.; Hellstrom, J.; De Waele, J. Petrographical and geochemical changes in bosnian stalagmites and their palaeo-environmental significance. *International Journal of Speleology* **2017**, *46*, 33-49.
53. Benson, A.; Hoffmann, D.L.; Bella, P.; Drury, A.J.; Hercman, H.; Atkinson, T.C. Building robust age models for speleothems – a case-study using coeval twin stalagmites. *Quaternary Geochronology* **2018**, *43*, 83-90.
54. Staubwasser, M.; Drăgușin, V.; Onac, B.P.; Assonov, S.; Ersek, V.; Hoffmann, D.L.; Veres, D. Impact of climate change on the transition of neanderthals to modern humans in europe. *Proceedings of the National Academy of Sciences* **2018**, *115*, 9116-9121.
55. Urban, J.; Margielewski, W.; Žák, K.; Hercman, H.; Sujka, G.; Mleczek, T. The calcareous speleothems in the pseudokarst jaskinia słowiańska-drwali cave, beskid niski mts., poland. *Nature Conservation* **2007**, *63*, 119-128.
56. Lindgren, A.; Hugelius, G.; Kuhry, P.; Christensen, T.R.; Vandenberghe, J. Gis-based maps and area estimates of northern hemisphere permafrost extent during the last glacial maximum. *Permafrost and Periglacial Processes* **2016**, *27*, 6-16.
57. Majorowicz, J. Permafrost at the ice base of recent pleistocene glaciations–inferences from borehole temperature profiles. **2012**, *5*, 7.
58. Błaszczyk, M.; Hercman, H.; Pawlak, J.; Gąsiorowski, M.; Matoušková, Š.; Aninowska, M.; Kicińska, D.; Tyc, A. Low to middle pleistocene paleoclimatic record from the kraków-częstochowa upland (poland) based on isotopic and calcite fabrics analyses. **2018**, *45*, 185.
59. Szewczik, J.; Nawrocki, J. Deep-seated relict permafrost in northeastern poland. *Boreas* **2011**, *40*, 385-388.
60. Pawlak, J.; Hercman, H. Numerical correlation of speleothem stable isotope records using a genetic algorithm. *Quaternary Geochronology* **2016**, *33*, 1-12.
61. Jex, C.N.; Baker, A.; Eden, J.M.; Eastwood, W.J.; Fairchild, I.J.; Leng, M.J.; Thomas, L.; Sloane, H.J. A 500 yr speleothem-derived reconstruction of late autumn–winter precipitation, northeast turkey. *Quaternary Research* **2011**, *75*, 399-405.
62. Badertscher, S.; Fleitmann, D.; Cheng, H.; Edwards, R.L.; Göktürk, O.M.; Zumbühl, A.; Leuenberger, M.; Tüysüz, O. Pleistocene water intrusions from the mediterranean and caspian seas into the black sea. *Nature Geoscience* **2011**, *4*, 236.
63. Demény, A.; Németh, A.; Kern, Z.; Czuppon, G.; Molnár, M.; Leél-Őssy, S.; Óvári, M.; Stieber, J. Recently forming stalagmites from the baradla cave and their suitability assessment for climate–proxy relationships. *Central European Geology* **2017**, *60*, 1-34.
64. Constantin, S.; Lauritzen, S.E.; Lundberg, J. New data on the chronology of the termination ii and paleoclimate during mis-5, based on the study of a stalagmite from closani cave (sw romania). *Archives of climate change in karst. Karst Waters Institute, Special Publication* **2006**, *10*, 98-100.

65. Siklósy, Z.; Demény, A.; Szenthe, I.; Leél-Őssy, S.; Pilet, S.; Lin, Y.; Shen, C.-C. Reconstruction of climate variation for the last millennium in the bükk mountains, northeast hungary, from a stalagmite record. *Quarterly Journal of the Hungarian Meteorological Service* **2009**, *113*, 245-263.
66. Tămaş, T.; Bojar, A.-V.; Constantin, S.; Lauritzen, S.-E. The δ18o record of a holocene stalagmite from v11 cave, nw romania. *Studia Universitatis Babe* **2007**, *57*, 77-79.
67. Siklósy, Z.; Demény, A.; LEÉL-ŐSSY, S.; Szenthe, I.; LAURITZEN, S.-E.; SHEN, C.-C. A cseppkövek kormeghatározása és azok paleoklimatológiai jelentősége. *Földtani Közlöny* **2011**, *141*, 1-100.
68. Onac, B.P.; Lauritzen, S. The climate of the last 150,000 years recorded inspeleothems: Preliminary results from north-western romania. *Theoretical and Applied Karstology* **1996**, *9*, 9-21.
69. Constantin, S.; Lauritzen, S.-E. Speleothem datings in sw romania. *Theoretical and Applied Karstology* **1998**, *11-12*, 35-45.
70. Surić, M.; Lončarić, R.; Lončar, N.; Bočić, N.; Bajo, P.; Columbu, A.; Drysdale, R.N.; Hellstrom, J.C. In *Eastern adriatic paleoenvironmental changes recorded from mis 10 to the recent in the modrič cave (croatia) speleothems–preliminary report*, Climate Change: The Karst Record, 8th International Conference KR8, 2017; 2017; p 105.
71. Demény, A.; Leél-Ossy, S.; Shen, C.-C.; Surányi, G. In *Middle pleistocene speleothem record from the baradla cave, northeast hungary*, EGU General Assembly Conference Abstracts, 2018; p 8894.
72. Riechelmann, D.F.C.; Schröder-Ritzrau, A.; Scholz, D.; Fohlmeister, J.; Spötl, C.; Richter, D.K.; Mangini, A. Monitoring bunker cave (nw germany): A prerequisite to interpret geochemical proxy data of speleothems from this site. *Journal of Hydrology* **2011**, *409*, 682-695.
73. Surić, M.; Lončarić, R.; Lončar, N.; Buzjak, N.; Bajo, P.; Drysdale, R.N. Isotopic characterization of cave environments at varying altitudes on the eastern adriatic coast (croatia) – implications for future speleothem-based studies. *Journal of Hydrology* **2017**, *545*, 367-380.
74. Surić, M.; Lončarić, R.; Bočić, N.; Lončar, N.; Buzjak, N. Monitoring of selected caves as a prerequisite for the speleothem-based reconstruction of the quaternary environment in croatia. *Quaternary International* **2018**, *494*, 263-274.
75. Surić, M.; Roller-Lutz, Z.; Mandić, M.; Bronić, I.K.; Juračić, M. Modern c, o, and h isotope composition of speleothem and dripwater from modrič cave, eastern adriatic coast (croatia). *International Journal of Speleology* **2010**, *39*, 4.
76. Drăguşin, V.; Balan, S.; Blamart, D.; Forray, F.L.; Marin, C.; Mirea, I.; Nagavciuc, V.; Orăşeanu, I.; Perşoiu, A.; Tîrlă, L., *et al.* Transfer of environmental signals from the surface to the underground at ascunsă cave, romania. *Hydrol. Earth Syst. Sci.* **2017**, *21*, 5357-5373.

 doi:10.20944/preprints201812.0038.v1

77. Ersek, V.; Onac, B.P.; Perșoiu, A. Kinetic processes and stable isotopes in cave dripwaters as indicators of winter severity. *Hydrological Processes* **2018**, *32*, 2856-2862.
78. Czuppon, G.; Bočić, N.; Buzjak, N.; Óvári, M.; Molnár, M. Monitoring in the barać and lower cerovačka caves (croatia) as a basis for the characterization of the climatological and hydrological processes that control speleothem formation. *Quaternary International* **2018**, *494*, 52-65.
79. Czuppon, G.; Demény, A.; Leél-Őssy, S.; Óvari, M.; Molnár, M.; Stieber, J.; Kiss, K.; Kármán, K.; Surányi, G.; Haszpra, L. Cave monitoring in the béke and baradla caves (northeastern hungary): Implications for the conditions for the formation cave carbonates. *International Journal of Speleology* **2018**, *47*, 2.
80. Fehér, K.; Kovács, J.; MáRKUS, L.; Borbás, E.; Tanos, P.; Hatvani, I.G. Analysis of drip water in an urban karst cave beneath the hungarian capital (budapest). *Acta Carsologica* **2016**, *45*, 213-231.
81. Domínguez-Villar, D.; Lojen, S.; Krklec, K.; Kozdon, R.; Edwards, R.L.; Cheng, H. Ion microprobe δ18o analyses to calibrate slow growth rate speleothem records with regional δ18o records of precipitation. *Earth and Planetary Science Letters* **2018**, *482*, 367-376.
82. Vreča, P.; Bronić, I.K.; Leis, A.; Demšar, M. Isotopic composition of precipitation at the station ljubljana (reaktor), slovenia–period 2007–2010. *Geologija* **2014**, *57*, 217-230.
83. Vodila, G.; Palcsu, L.; Futó, I.; Szántó, Z. A 9-year record of stable isotope ratios of precipitation in eastern hungary: Implications on isotope hydrology and regional palaeoclimatology. *Journal of Hydrology* **2011**, *400*, 144-153.
84. Holko, L.; Dóša, M.; Michalko, J.; Šanda, M. Isotopes of oxygen-18 and deuterium in precipitation in slovakia / izotopy kyslíka-18 a deutéria v zrážkach na slovensku. **2012**, *60*, 265.
85. Rozanski, K.; Araguás-Araguás, L.; Gonfiantini, R. Isotopic patterns in modern global precipitation. In *Climate change in continental isotopic records*, . Ed. American Geophysical Union: 1993; pp 1-36.
86. Rozanski, K.; Sonntag, C.; Münnich, K.O. Factors controlling stable isotope composition of european precipitation. *Tellus* **1982**, *34*, 142-150.
87. Vreča, P.; Bronić, I.K.; Horvatinčić, N.; Barešić, J. Isotopic characteristics of precipitation in slovenia and croatia: Comparison of continental and maritime stations. *Journal of Hydrology* **2006**, *330*, 457-469.
88. O'Neil, J.R.; Taylor, H.P. Oxygen isotope equilibrium between muscovite and water. *Journal of Geophysical Research* **1969**, *74*, 6012-6022.
89. Jex, C.N.; Baker, A.; Fairchild, I.J.; Eastwood, W.J.; Leng, M.J.; Sloane, H.J.; Thomas, L.; Bekaroğlu, E. Calibration of speleothem δ18o with instrumental climate records from turkey. *Global and Planetary Change* **2010**, *71*, 207-217.
90. Vreča, P.; Bronić, I.K.; Leis, A. Isotopic composition of precipitation at the station portorož,, slovenia–period 2007–2010. *Geologija* **2015**, *58*, 233-246.

Preprints (www.preprints.org) | NOT PEER-REVIEWED | Posted: 4 December 2018 doi:10.20944/preprints201812.0038.v1

91. Golobočanin, D.; Ogrinc, N.; Bondzić, A.; Miljević, N. Isotopic characteristics of meteoric waters in the belgrade region. *Isotopes in Environmental and Health Studies* **2007**, *43*, 355-367.
92. Dublyansky, Y.V.; Klimchouk, A.B.; Tokarev, S.V.; Amelichev, G.N.; Langhamer, L.; Spötl, C. Stable isotopic composition of atmospheric precipitation on the crimean peninsula and its controlling factors. *Journal of Hydrology* **2018**, *565*, 61-73.
93. Demircan, M.; Yiğitbaşioğlu, H. In *Precipitation's fingerprint and it's usage in paleoclimatology*, VIII Geographical Symposium, Ankara, Turkey, 23-24.10.2014, 2014; Turkish State Meteorological Service: Ankara, Turkey, 2014; pp 50-59.
94. Dorale, J.A.; Liu, Z. Limitations of hendy test criteria in judging the paleoclimatic suitability of speleothems and the need for replication. *Journal of Cave and Karst Studies* **2009**, *71*, 73-80.
95. McDermott, F.; Atkinson, T.C.; Fairchild, I.J.; Baldini, L.M.; Mattey, D.P. A first evaluation of the spatial gradients in δ18o recorded by european holocene speleothems. *Global and Planetary Change* **2011**, *79*, 275-287.
96. Poage, M.A.; Chamberlain, C.P. Empirical relationships between elevation and the stable isotope composition of precipitation and surface waters: Considerations for studies of paleoelevation change. *American Journal of Science* **2001**, *301*, 1-15.
97. Krajcar-Bronić, I.; Horvatinčić, N.; Obelić, B. Two decades of environmental isotope records in croatia: Reconstruction of the past and prediction of future levels. *Radiocarbon* **1998**, *40*, 399-416.
98. Hunjak, T.; Lutz, H.O.; Roller-Lutz, Z. Stable isotope composition of the meteoric precipitation in croatia. *Isotopes in Environmental and Health Studies* **2013**, *49*, 336-345.
99. Mezga, K.; Urbanc, J.; Cerar, S. The isotope altitude effect reflected in groundwater: A case study from slovenia. *Isotopes in Environmental and Health Studies* **2014**, *50*, 33-51.
100. Dotsika, W.; Poutoukis, D.; Raco, B.; Psomiadis, D. Stable isotope composition of hellenic bottled waters. *Journal of Geochemical Exploration* **2010**, *107*, 299-304.
101. Lechleitner, F.; Amirnezhad-Mozhdehi, S.; Columbu, A.; Comas-Bru, L.; Labuhn, I.; Pérez-Mejías, C.; Rehfeld, K. The potential of speleothems from western europe as recorders of regional climate: A critical assessment of the sisal database. *Preprints* **2018**.
102. Žák, K.; Urban, J.; Cílek, V.; Hercman, H. Cryogenic cave calcite from several central european caves: Age, carbon and oxygen isotopes and a genetic model. *Chemical Geology* **2004**, *206*, 119-136.
103. Richter, D.K.; Riechelmann, D.F.C. Late pleistocene cryogenic calcite spherolites from the malachitdom cave (ne rhenish slate mountains, germany): Origin, unusual internal structure and stable co isotope composition. *International Journal of Speleology* **2008**, *37*, 5.
104. Zak, K.; Hercman, H.; Orvosova, M.; Jackova, I. Cryogenic cave carbonates from the cold wind cave, nízke tatry mountains, slovakia: Extending the age range of

Preprints (www.preprints.org) | NOT PEER-REVIEWED | Posted: 4 December 2018 doi:10.20944/preprints201812.0038.v1

cryogenic cave carbonate formation to the saalian. *International Journal of Speleology* **2009**, *38*, 139-152.

105. Žák, K.; Richter, D.K.; Filippi, M.; Živor, R.; Deininger, M.; Mangini, A.; Scholz, D. Coarsely crystalline cryogenic cave carbonate – a new archive to estimate the last glacial minimum permafrost depth in central europe. *Clim. Past* **2012**, *8*, 1821-1837.
106. Žák, K.; Onac, B.P.; Perşoiu, A. Cryogenic carbonates in cave environments: A review. *Quaternary International* **2008**, *187*, 84-96.
107. Orvošová, M.; Deininger, M.; Milovský, R. Permafrost occurrence during the last permafrost maximum in the western carpathian mountains of slovakia as inferred from cryogenic cave carbonate. *Boreas* **2014**, *43*, 750-758.
108. NGRIP, N.G.I.C.P.m. High-resolution record of northern hemisphere climate extending into the last interglacial period. *Nature* **2004**, *431*, 147-151.
109. Sanchi, L.; Ménot, G.; Bard, E. Insights into continental temperatures in the northwestern black sea area during the last glacial period using branched tetraether lipids. *Quaternary Science Reviews* **2014**, *84*, 98-108.
110. Vermeesch, P. On the visualisation of detrital age distributions. *Chemical Geology* **2012**, *312-313*, 190-194.